Capture cross sections of ^{15}N(n, γ)^{16}N at astrophysical energies*

Guang-Wei Fan(樊广伟)[1;1)] Jun-Bing Ma(马军兵)[2] Zong-Qiang Sheng(圣宗强)[1]
Guo-Zhu Shi(石国柱)[2] Feng Tian(田丰)[3] Jun Wang(王军)[1] Chao Zhang(张超)[1]

[1] School of Chemical Engineering, Anhui University of Science and Technology, Huainan 232001, China
[2] Institute of Modern Physics, Chinese Academy of Sciences, Lanzhou 730000, China
[3]Shanghai Institute of Applied Physics, Chinese Academy of Sciences, Shanghai 201800, China

Abstract: We have reanalyzed reaction cross sections of ^{16}N on a ^{12}C target. The nucleon density distribution of ^{16}N, especially surface density distribution, was extracted using the modified Glauber model. On the basis of dilute surface densities, the ^{15}N(n, γ)^{16}N reaction is discussed within the framework of the direct capture reaction mechanism. The calculations agree quite well with the experimental data.

Keywords: capture cross sections, reaction cross sections, ^{15}N(n, γ)^{16}N, Glauber model, direct capture

PACS: 25.40.Lw, 26.20.+f, 25.70.Mn, 21.10.Gv **DOI:** 10.1088/1674-1137/40/12/124101

1 Introduction

Nuclear reactions at low energies play a crucial role in nuclear astrophysics. Often the reactions are quite difficult to measure in laboratories; the theoretical extrapolation is important in studies [1–4]. The ^{15}N(n, γ)^{16}N reaction is such a low-energy reaction. Its cross section (σ_c) at astrophysical energies is an important input in the reaction network for the determination of heavier neutron-rich elements $A > 16$ in both inhomogeneous big bang and in red giant environments. Besides, it is a competition reaction to the reaction ^{15}N(α, γ)^{19}F. ^{19}F is a key element for evolutionary studies in the asymptotic giant branch stars in which the ^{15}N(n, γ)^{16}N reaction largely affect the abundance of ^{19}F [5–7].

The experimental σ_c of the ^{15}N(n, γ)^{16}N reaction is of considerable uncertainty. In 1996, Meissner et al. [8] measured the σ_c at neutron energies of 25, 152, and 370 keV. The authors performed direct capture calculations to interpret the measurements, but a large gap appears between the calculations and the experimental data. Thus, further theoretical studies are necessary. In the process of the ^{15}N(n, γ)^{16}N reaction, a free neutron in the continuum state is captured by the ^{15}N target and finally stays in a ground state of the compound nucleus ^{16}N. The reaction is mostly determined by the spectroscopic factors, the nuclear structure properties of four low-lying states in ^{16}N, and the effective interaction potential between the free neutron and the ^{15}N target. As for the spectroscopic factors, Bohne et al. [9] and Bardayan et al. [10] measured the angular distributions of the ^{15}N(d, p)^{16}N reaction, and Guo et al. [11] measured the angular distributions of the ^{15}N(^{7}Li, ^{6}Li)^{16}N reaction. These groups obtained the spectroscopic factors, respectively. Although a recent experiment and analysis for ^{15}N(n, γ)^{16}N by Guo et al. gives a more accurate calculation of this reaction in the energy regime of interest, it is still meaningful to explore the errors from the structure of ^{16}N. Neelam et al. [12] discuss the structure effects of this reaction from the Coulomb dissociation of ^{16}N. They suggest an indirect method to measure the cross sections of ^{15}N(n, γ)^{16}N. Fan et al. [13] have proved that the low-lying states structure in ^{8}Li and the interaction potential between ^{7}Li and free neutrons can be explored by the reaction cross section (σ_R) of ^{8}Li on stable targets. In this paper, we will analyze the errors of ^{15}N(n, γ)^{16}N according to the low-lying state structure of ^{16}N deduced from σ_R of ^{16}N on a ^{12}C target.

2 Theoretical mechanism

The Glauber model is a powerful tool to extract the nuclear surface structure by fitting the experimental σ_R. The model is based on the independent individual nucleon-nucleon (N-N) collisions in the overlap zone of the colliding nuclei, which account for a significant part of the breakup effects. It successfully explains the observed σ_R for various systems [14, 15]. The model will be employed in this article to deduce the surface structure

Received 17 February 2016, Revised 9 July 2016

* Support given by National Natural Science Foundation of China (11447236, 11505002, 11247001) and Foundation of Anhui University of Science and Technology (11130, 12608)

1) E-mail: gwfan@aust.edu.cn

of ^{16}N and interaction potential of incident neutron on the ^{15}N core. The Glauber model is a standard calculation, and details can be found in a number of references, e.g. Refs. [16–18].

On the basis of the experimental spectroscopic factors, surface structure of ^{16}N, and the interaction potential, the direct capture theory will be utilized to calculate the σ_c of the reaction ^{15}N(n, γ)^{16}N [19]. In the theory the neutron in a continuum state is captured by a target nucleus ^{15}N that goes to a composite nucleus ^{16}N via a transition with an E1 electric dipole. The σ_c is given by

$$\sigma^{\mathrm{E1}}_{^{15}\mathrm{N}\to{}^{16}\mathrm{N}}=\frac{16\pi}{9\hbar}\kappa_\gamma^3\left|Q^{\mathrm{E1}}_{^{15}\mathrm{N}\to{}^{16}\mathrm{N}}\right|, \tag{1}$$

where $\kappa_\gamma=\dfrac{E_\gamma}{\hbar c}$ is the wave number that corresponds to a γ-ray energy E_γ. $Q^{\mathrm{E1}}_{^{15}\mathrm{N}\to{}^{16}\mathrm{N}}$ transition matrix element given by

$$Q^{\mathrm{E1}}_{^{15}\mathrm{N}\to{}^{16}\mathrm{N}}=\psi_c\left|O^{\mathrm{E1}}\right|\psi_c, \tag{2}$$

where O^{E1} stands for the electric dipole operator. The initial state wave function ψ_c is the incoming neutron wave function, and the wave function ψ_b represents the bound state of the composite nucleus ^{16}N. The wave functions necessary in the direct theory will be obtained by solving the scattering and bound-state systems, respectively, for a given interaction potential. Thus, the essential ingredients are the potentials used to generate the wave functions ψ_c and ψ_b and the normalization given by the spectroscopic factor.

3 Nuclear structure of ^{16}N

Ozawa et al. [20] and Fang et al. [21] have measured the σ_R of ^{16}N on a ^{12}C target, analyzed the experimental data with standard Glauber model, and obtained the density distribution of ^{16}N. Unfortunately, there is a 10% – 20% underestimation in the standard Glauber model between the experimental σ_R and the theoretical calculations at intermediate energies [22]. Although the density distribution has been extracted, it is necessary to reanalyze the experimental data with a modified Glauber model [23]. The Glauber model requires the structure information, namely, the density distribution of the projectile and target. The proper target density is employed from electron-scattering experimental data, which is converted to matter densities by unfolding the proton charge density while taking into account the quadrupole deformation. ^{16}N is divided into two parts for small separation energy of last neutron $E_{1n}=2.491$ MeV: ^{15}N core and a valence neutron part. The harmonic oscillator-(HO-) type function is chosen as the initial function of the core. The single-particle model (SPM) function is chosen as the initial shape of the valence neutron part.

The SPM function is a realistic model to describe the tail structure. The wave function of the valence neutron is calculated by solving the Schrödinger equation numerically with a Woods-Saxon potential. The SPM takes into account the Coulomb and the centrifugal barrier effects. The main equations of the functions are expressed as a.

HO type function

$$\rho_c^{\mathrm{i}}(r)=\rho_{c0}^{\mathrm{i}}\times\left(1+\frac{C-2}{3}\left(\frac{r}{b}\right)^2\right)\exp\left(-\left(\frac{r}{b}\right)^2\right), \tag{3}$$

where i denotes the proton or neutron, C is the number of protons or neutrons in the core, b is the width of the core, and ρ_{c0} is the normalization factor. The same width is used for the proton- and neutron-core density distributions.

The Woods-Saxon potential is of the form

$$V=\left(-V_0+V_1(l\cdot s)\frac{r_{l\cdot s}^2}{r}\right)\left[1+\exp\left(\frac{r-R_c}{a}\right)\right]^{-1}, \tag{4}$$

where a is the diffuseness parameter, $R_c(=r_0A^{1/3}$, A is the nuclear mass number) is the radius of the Woods-Saxon potential, $r_{l\cdot s}$ (= 1.1 fm) is the radius for spin orbit potential, and V_1 (= 10 MeV) is the $l_{l\cdot s}$ strength. The depth of the potential V_0 is adjusted to reproduce the experimental separation energy of the valence neutron.

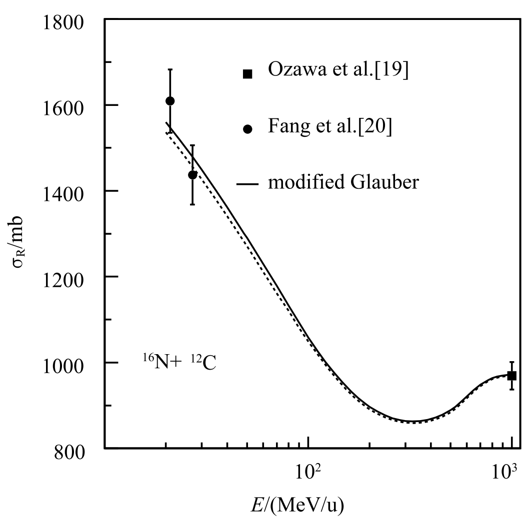

Fig. 1. The energy dependent σ_R of ^{16}N on ^{12}C. The solid curve denotes the theoretical fit of this work. The dashed line denotes the calculation with $a_0=0.60$ fm and $r_0=1.20$ fm.

Figure 1 shows the energy dependent σ_R of ^{16}N on ^{12}C target. The best-fit is shown by a solid curve; the reduced χ^2 for the best-fit is 0.55, which means a reasonable fit. The width of the HO function is $b=1.551\pm0.055$ fm, and the interaction parameters of the potential are $a_0=0.65\pm0.13$ fm, $r_0=1.25\pm0.14$ fm.

The errors are determined by the method of fit with total χ^2+1. The matter radius of ^{16}N equals (2.385±0.091) fm; it is the low limit of the radii given by previous work through the standard Glauber model, thereby calling for the reanalysis. The difference is easily understandable, because the standard Glauber model underestimates the σ_R, thus a larger density is needed to fill the gap. Figure 2 lists the radius of ^{16}N. The dashed line in Fig. 1 shows the calculation with a_0 = 0.60 fm and r_0 = 1.20 fm. The reduced χ^2 is 0.95. The difference between the best-fit is limited in the low energy region. It is because the potential parameters determine the surface structure of ^{16}N. The difference at 30 MeV/u is about 2%. It is large enough to illustrate the appropriateness of using reaction cross-sections to discuss the capture cross-sections.

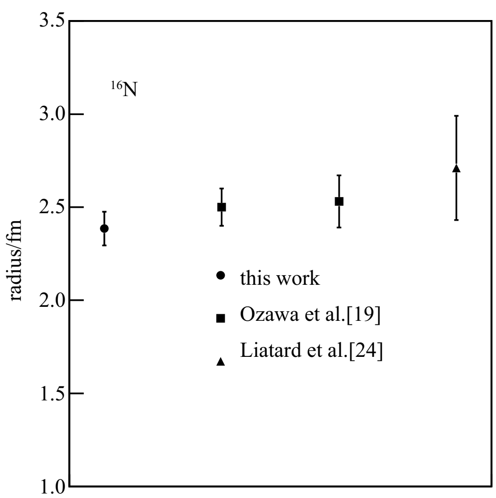

Fig. 2. Radius of ^{16}N. The present result is presented by solid circle. The other results are represented by solid squares [19] and solid triangles [24].

4 Cross sections of ^{15}N (n, γ)^{16}N

The direct capture for this reaction is dominated by the p→d wave transition to the ground state, p→s wave transition to the first excited state at 0.120 MeV, p→d wave transition to the second excited state at 0.296 MeV, and p→s wave transition to the third excited state at 0.397 MeV of ^{16}N. The γ-ray transitions are all dominated by the E1 multipolarity. The $J_b = 2^-$ ground state ($J_b = 0^-$ 1st excited state, $J_b = 3^-$ 2nd excited state, $J_b = 1^-$ 3rd excited state) in ^{16}N is described as a $j_b = d_{5/2}$ neutron ($j_b = s_{1/2}$ neutron, $j_b = d_{5/2}$ neutron, $j_b = s_{1/2}$ neutron) coupled to the ^{15}N core, which has an intrinsic spin $I_x = 1/2^-$. Actually, Meissner et al. [8] and Huang et al. [26] have all given detailed explanations on the reaction. We will only discuss the errors from the low-lying state of ^{16}N.

In the calculation, the latest experimental spectroscopic factors by Guo et al. are employed. Their values are SF = 0.96 ± 0.09 for the ground state, SF = 0.69 ± 0.09 for the 2^- state, SF = 0.84 ± 0.08 for the 3^- state, and SF = 0.65 ± 0.08 for the 1^- state. The wave function ψ_b of low-lying states in ^{16}N are calculated numerically in the direct capture theory with a_0 =0.65 ± 0.13 fm and b =1.25 ± 0.14 fm obtained in Section 3. The parameters for computing the incoming neutron wave function ψ_c are determined with the ANC method [27–29], as suggested by Huang et al. The calculated ANC value equals 0.85 fm$^{-1/2}$ for the ground state of ^{16}N, 1.10 fm$^{-1/2}$ for the first excited state, 0.29 fm$^{-1/2}$ for the second excited state, and 1.08 fm$^{-1/2}$ for the third excited state.

Figure 3 shows the σ_c of ^{15}N + n. The dash-dot-dot and dash-dot lines denote the p→d wave transition to the ground and the second excited states respectively; dotted and dashed lines denote the p→s transition to the first and third excited states, respectively. The solid line is the summation of the four transitions. The shaded area shows the error due to the nuclear properties of ^{16}N; it is a little higher at 12% compared to that of ^{7}Li (n, γ)^{8}Li [13]. There are two main reasons, as follows: (a) the same potential parameters are employed to calculate wave functions of ^{16}N low-lying states without considering the influence of valence neutron on the ^{15}N core in different states of ^{16}N; (b) the number of existing experimental measurements of σ_R is not enough to extracted the structure information - the data at intermediate energies ∼100 MeV/u are required; (c) the existing σ_R contain contributions of excited states, especially the first excited state - the first state in ^{16}N, which has a lifetime of 5.25 μs, can reach the reaction target in the transition method. In order to solve the questions noted above, new measurements of the σ_R of ^{16}N are required on stable targets.

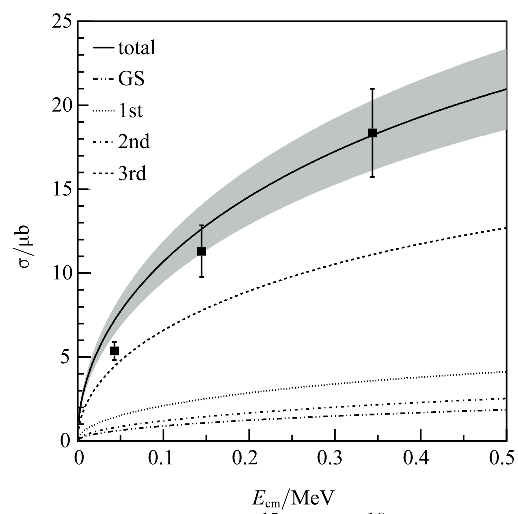

Fig. 3. Cross sections of ^{15}N (n, γ)^{16}N. The shaded area indicate the error caused by structure of ^{16}N, and the experimental data are from Ref. [8].

5 Conclusion

We reanalyzed the reaction cross section of ^{16}N on a ^{12}C target with modified Glauber model and extracted its structure information. The ^{15}N + n reaction has been discussed by means of the structure. Although more accurate cross sections have not been obtained, the article found some problems and their resolution.

References

1 C. Rolfs and W. Rodney, *Cauldrons in the Cosmos* (University of Chicago Press, Chicago, 1988)

2 L. H. Kawano, W. A. Fowler, R. W. Kavanagh et al, Astrophys. J, **372**: 1 (1991)

3 J. C. Blackmon, A. E. Champagne, J. K. Dickens et al, Phys. Rev. C, **54**: 383–388 (1996)

4 S. Burles, K. M. Nollett, J. W. Truran et al, Phys. Rev. Lett., **82**: 4176 (1999)

5 S. E. Woosley, D. H. Hartmann, R. D. Ho_man et al, Astrophys. J., **356**: 272 (1990)

6 M. Forestini, S. Goriely, A. Jorissen et al, Astron. Astrophys, **261**: 157 (1992)

7 A. Jorissen, V. V. Smith, and D. L. Lambert, Astron. Astrophys, **261**: 164 (1992)

8 J. Meissner, H. Schatz, H. Herndl et al, Phys. Rev. C, **53**: 977 (1996)

9 W. Bohne, J. Bommer, H. Fuchs et al, Nucl. Phys. A, **196**: 41 (1972)

10 D. W. Bardayan et al, Phys. Rev. C, **78**: 052801(R) (2008)

11 B. Guo, Z. H. Li, Y. J. Li et al, Phys. Rev. C, **89**: 012801(R) (2014)

12 Neelam, Shubhchintak, and R. Chatterjee, Phys. Rev. C, **92**: 044615 (2015)

13 G. W. Fan, M. Fukuda, D. Nishimura et al, Phys. Rev. C, **91**: 014614 (2015)

14 I. Tanihata et al, Phys. Rev. Lett, **55**: 2676 (1985)

15 A. Ozawa, T. Suzuki and I. Tanihata, Nucl. Phys. A, **693**: 32–62 (2001)

16 R. J. Glauber, *Lectures in Theoretical Physics*. Edited by W. E. Brittin, L. G. Dunham. (New York: Interscience, 1959), p.1: 315

17 X. Z. Cai et al, Chin. Phys. Lett, **17**: 565 (2000)

18 M. Fukuda et al, Phys. Lett. B, **268**: 339 (1991)

19 C. A. Bertulani, Computer Physics Commun., **156**: 123 (2003)

20 A. Ozawa et al, Nucl. Phys. A, **691**: 599 (2001)

21 D. Q. Fang et al, Phys. Rev. C, **61**: 064311 (2000)

22 M. Takechi, M. Fukuda, M. Mihara et al, Eur. Phys. J. A, **25**: 217–219 (2005)

23 M. Takechi, M. Fukuda, M. Mihara et al, Phys. Rev. C, **79**: 061601(R) (2009)

24 A. Bohr and B. R. Mottelson, *Nuclear Structure*, Vol. I (Benjamin, New York, 1975)

25 E. Liatard et al, Europhys. Lett, **13**: 401 (1990)

26 J. T. Huang, C. A. Bertulani, and V. Guimaraes, At. Data Nucl. Data Tables, **96**: 824 (2010)

27 P. Navratil, C.A. Bertulani, and E. Caurier, Phys. Lett. B, **634**: 191 (2006)

28 P. Navratil, C.A. Bertulani, and E. Caurier, Phys Rev, C, **73**: 065801(2006)

29 Sofia Quaglioni and Petr Navratil, Phys. Rev. Lett, **101**: 092501 (2008)